Available online at www.sciencedirect.com
SCIENCE DIRECT
Carbohydrate Polymers 58 (2004) 345–358
Carbohydrate Polymers
www.elsevier.com/locate/carbpol

DSC and NMR relaxation studies of starch–water interactions during gelatinization

Kanitha Tananuwong[1], David S. Reid*

Department of Food Science and Technology, University of California, Davis, 1 Shields Avenue, Davis, CA 95616, USA

Received 30 July 2003; revised 24 June 2004; accepted 3 August 2004
Available online 11 September 2004

Abstract

The interactions between water and starch during gelatinization as affected by water content, maximum heating temperature and amylopectin crystallinity pattern were investigated by Differential Scanning Calorimetry (DSC) and ^{1}H NMR relaxation. DSC was used to measure additional unfrozen water (AUW) arising from gelatinization, reflecting enhanced water–starch interactions, and enthalpy of gelatinization (ΔH_{gel}) of waxy corn, normal corn, potato and pea starches between 0.7 and 3.0 g water/g dry starch. The contribution of separated G and M1 stages in gelatinization was estimated using a deconvolution DSC technique. The results show that AUW largely depends on the initial water content. For the samples subjected to higher heating temperature (M1 process), a larger AUW is found presumably due to the greater disruption in granule structure. Deconvolution of the biphasic endotherm suggests that, as water content increases, the M1 process is much reduced and gradually incorporates into the dominant G process. NMR T_2 distribution reveals two distinct water populations corresponding to intra- and extra-granular water, which rapidly exchange during gelatinization. After the M1 process, a relatively homogeneous gel with one water fraction from fast diffusional averaging is obtained. AUW and peak T_2 values of pea starch are intermediate between those of native corn and potato starches, consistent with its composite A- and B-type crystal structure.

Keywords: Starch; Water; Gelatinization; Differential scanning calorimetry; Nuclear magnetic resonance; Deconvolution; Unfrozen water; Enthalpy of gelatinization; Spin–spin relaxation time

1. Introduction

In addition to providing a major source of energy in food products, starch plays a crucial role in textural modification via a process called 'gelatinization', the break up and partial dissolution of the starch granule upon heating in the presence of water (Thomas & Atwell, 1999). In order to optimize processing operations and obtain desired quality of starch-based foods, a thorough understanding of starch gelatinization is required. Although there have been many studies on starch gelatinization, there is still little information on the interactions between starch and water, which play a key role in the gelatinization mechanism.

Starch–water interactions can be monitored by following the change in physical state of water. One approach is to measure the amount of unfrozen water (UW), the water within a system, which does not freeze out as ice at subfreezing temperature. This group of water molecules has been proposed to be associated in some way more closely with the solute molecules although it may not be totally immobilized or 'bound' (Franks, 1986; Li, Dickinson, & Chinachoti, 1998). The amount of frozen water (FW) and UW in polymer systems has been extensively investigated by Differential Scanning Calorimetry (DSC) (Li et al., 1998; Roman-Gutierrez, Guilbert, & Cuq, 2002; Wootton & Bamunuarachchi, 1978). The dynamics of water–starch interactions can also be studied by NMR relaxation. Several ^{1}H and ^{17}O NMR studies have revealed a drastic decrease in spin–spin relaxation time (T_2) of starch in excess water or D_2O within the gelatinization temperature range, suggesting an increase in the extent of hydration of starch polymers (Cheetam & Tao, 1998a; Chinachoti, White, Lo, & Stengle,

* Corresponding author. Tel.: +1-530-752-8448; fax: +1-530-752-4759.
E-mail addresses: ktwong@ucdavis.edu (K. Tananuwong), dsreid@ucdavis.edu (D.S. Reid).
[1] Tel.: +1-530-752-7112; fax: +1-530-752-4759.

0144-8617/$ - see front matter © 2004 Elsevier Ltd. All rights reserved.
doi:10.1016/j.carbpol.2004.08.003

1991; Lelievre & Mitchell, 1975). Those studies reported only one T_2 value which represents an average between the T_2 of bulk and surface water, based on the two-state fast-exchange model. However, from the continuous T_2 distribution pattern, multiple T_2 values of water protons were recently reported for starch–water mixtures, reflecting the microscopic distribution of water in the system (Chatakanonda, Dickinson, & Chinachoti, 2003; Tang, Godward, & Hills, 2000). Dynamic redistribution between extra- and intra-granular water of potato starch was followed by monitoring a change in the continuous distribution of T_2 components (Chatakanonda, Chinachoti et al., 2003; Tang, Brun, & Hills, 2001). Therefore, the use of a water compartmentalization concept helps to provide insight into the nature of starch–water interactions.

Starch gelatinization is influenced by a number of parameters, including temperature and water content. According to the DSC studies, during heating of a starch–water mixture, two endothermic peaks related to the gelatinization process, identified as G and M1 (Donovan, 1979), may be seen in the thermogram. For samples of the same size heated at the same rate, the enthalpy of the G and M1 peaks as well as the position of the M1 peak are dependent on the water content (Donovan, 1979; Hoseney, Zeleznak & Yost, 1986; Rolee & LeMeste, 1999). The mechanism underlying these phenomena is still under debate. Information on how water interacts with starch during the G and M1 endothermic processes is also scant. Starches containing different amylopectin crystallinity patterns and/or amylose–amylopectin ratios also exhibit different gelatinization behaviors. (Jenkins & Donald, 1998; Matveev et al., 2001; Yuryev, Kalistratova, van Soest, & Niemann, 1998). It is also interesting to study the interactions between water and starches with different microstructures, which may provide better understanding on their different gelatinization behaviors.

The aim of this work is to investigate effects of water content, maximum heating temperature and amylopectin crystallinity pattern on the interactions between starch and water during gelatinization, using a deconvoluted DSC technique and proton NMR relaxation. Information obtained from this study should help to clarify the mechanism of starch gelatinization. Since the interactions between starch and water also influence the starch functionality, a better understanding of those interactions could provide a basis for modifying starch functional properties as well as improving quality of starch-based food.

2. Material and methods

2.1. Sample preparation

Waxy corn, normal (wild-type) corn and potato starch were purchased from Sigma–Aldrich, Inc. (St Louis, MO). Smooth pea starch (Accu-Gel) was obtained from Parrheim Foods (Manitoba, Canada). In order to ensure a uniform water distribution in low water content samples (0.7–0.9 g water/g dry starch), 1 g of starch with approximately 10% initial moisture content was thoroughly mixed with the required amount of water in a vial. This mixture was equilibrated overnight before loading into either a preweighed DSC volatile sample pan or a 5 mm NMR sample tube. For samples with higher water content (1.0– 3.0 g water/g dry starch), a known weight of the starch (10% moisture) was directly placed in a DSC volatile sample pan or an NMR sample tube, and water was added. The pan or tube was sealed, reweighed and equilibrated for 24 h before the experiment. The approximate weights of the starch–water mixture in DSC pans and NMR tubes were 15 and 500 mg, respectively. For the DSC study, the exact water content was confirmed after collecting the calorimetric data.

2.2. Deconvolution DSC technique

A DSC (Pyris 1, Perkin Elmer, Norwalk, CT) with Pyris™ operation software was used for the determination of FW, UW, additional unfrozen water (AUW) resulting from gelatinization and enthalpy of gelatinization (ΔH_{gel}) in the starch–water systems. The calorimeter was equipped with an Intracooler 2P (Perkin Elmer, Norwalk, CT) and nitrogen gas purge. An empty volatile sample pan was used as a reference.

It has been shown that, when the heating process was stopped partway through the endotherm and the sample was cooled down, the portion of the sample that had not yet undergone a phase transition on the first heating was observed to go through the transition on the second heating (Donovan, 1979). Hence, by stopping the heating process at the temperature at which the interactions underlying the G endotherm should be just completed (the peak temperature of the G endotherm), the G and the M1 endotherm could be deconvoluted. The deconvolution DSC procedure is illustrated in Fig. 1a. In each set, several scans were performed on the same sample. The DSC scan was stopped either at the temperature near the peak temperature of the G endotherm (T1) or slightly above the conclusion temperature of the overall gelatinization endotherm (T2). T1 and T2 are different depending on the initial water content and the starch type, as listed in Table 1. Typical sets of scans from the DSC program are shown in Fig. 1b and c. The illustration of successful separation of the G and the M1 endotherm is in Fig. 2. All measurements were done in triplicate. On completion of the experiment sequence in Fig. 1a, the volatile sample pan was punctured and dried overnight in an oven at 115 °C, then reweighed to determine the exact water content in the sample.

Based on the known heat of fusion of ice of 334.7 J/g, FW (g water/g dry starch) was calculated from the area under the ice melting endotherm. AUW arising from gelatinization was calculated as the difference between

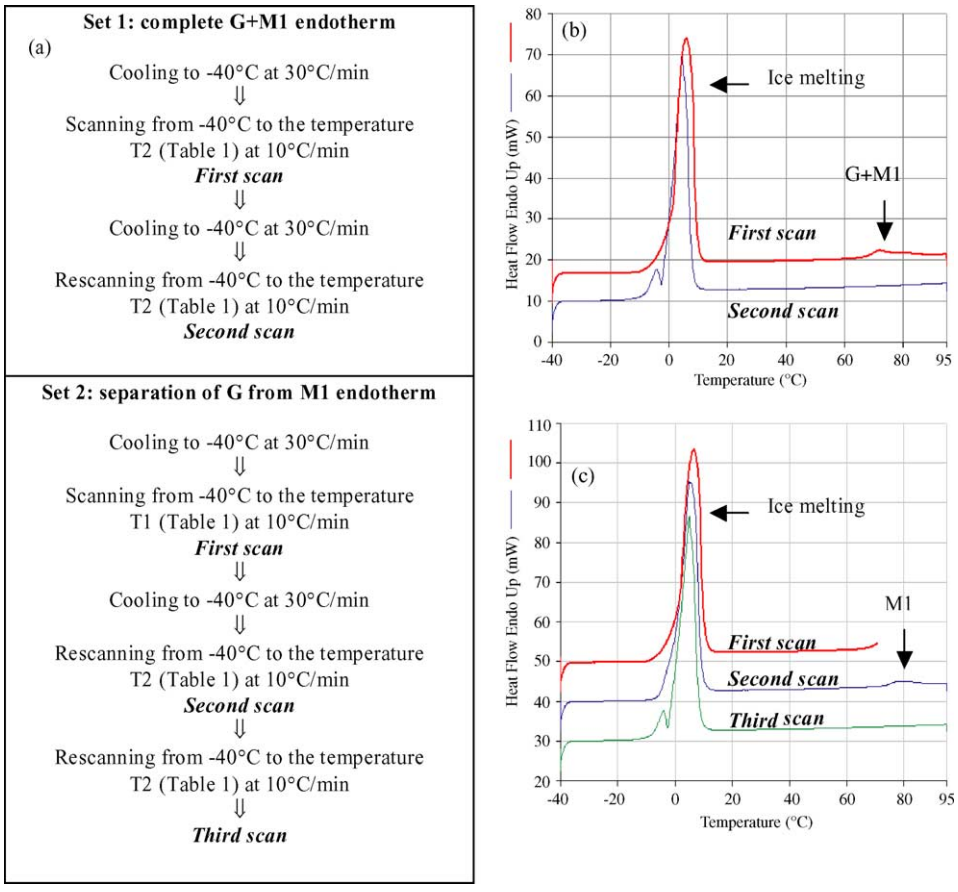

Fig. 1. Description of the DSC experiment: (a) flow chart for deconvolution DSC technique; (b) and (c) DSC scans of waxy corn starch, 1.3 g water/g dry starch, using the temperature program in sets 1 and 2, respectively.

FW of sequential scans.

$$AUW_G = FW_{1st\ scan,set\ 2} - FW_{2nd\ scan,set\ 2} \quad (1)$$

$$AUW_{M1} = FW_{2nd\ scan,set\ 2} - FW_{3rd\ scan,set\ 2} \quad (2)$$

$$AUW_{G+M1} = FW_{1st\ scan,set\ 1} - FW_{2nd\ scan,set\ 1} \approx AUW_G + AUW_{M1} \quad (3)$$

where AUW_G, AUW_{M1} and AUW_{G+M1} are AUW (g water/g dry starch) resulting from the G endotherm, the M1 endotherm, and the complete gelatinization, respectively.

ΔH_{gel} (J/g dry starch) was calculated from the area under the gelatinization endotherms. ΔH_{gel} of the complete gelatinization ($\Delta H_{gel,G+M1}$), and that of the M1 endotherm ($\Delta H_{gel,M1}$) were calculated from the first scan in set 1

Table 1
Target temperatures used in the DSC temperature programs in Fig. 1a

Water content (g water/g dry starch)	Target temperatures (°C) related to the gelatinization endotherms							
	Waxy corn		Normal corn		Potato		Pea	
	T1[a]	T2[b]	T1	T2	T1	T2	T1	T2
0.70	72.5	110.0	72.5	110.0	64.0	105.0	71.5	120.0
0.90	72.5	105.0	72.5	105.0	64.0	100.0	71.5	115.0
1.10	72.5	100.0	72.5	95.0	64.0	95.0	71.5	110.0
1.30	72.5	95.0	72.5	95.0	64.0	90.0	71.5	105.0
1.50	72.5	90.0	72.5	90.0	64.0	90.0	71.5	100.0
1.75	72.5	90.0	72.5	85.0	64.0	85.0	71.5	95.0
2.00	72.5	90.0	72.5	85.0	64.0	80.0	71.5	95.0
2.50	72.5	90.0	72.5	85.0	64.0	80.0	71.5	90.0
3.00	72.5	90.0	72.5	85.0	64.0	80.0	71.5	90.0

[a] Temperature near the peak temperature of the first endotherm (G endotherm).
[b] Temperature slightly above the conclusion temperature of the overall gelatinization endotherms.

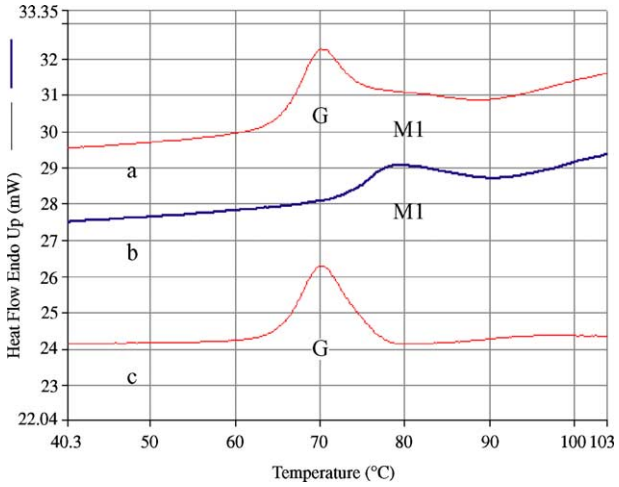

Fig. 2. DSC thermogram of normal corn starch–water mixtures, 1.1 g water/g dry starch, illustrating separation of the G and the M1 endotherm using deconvolution technique in Fig. 1a: (a) biphasic endotherm from the first scan in set 1; (b) the second scan in set 2 showing only M1 endotherm; (c) deconvolution of the G endotherm by subtracting b from a.

and the second scan in set 2 (Fig. 1a), respectively. ΔH_{gel} of the G endotherm ($\Delta H_{gel,G}$) was then calculated as the difference

$$\Delta H_{gel,G} = \Delta H_{gel,G+M_1} - \Delta H_{gel,M1} \quad (4)$$

Conventional mathematical deconvolution was performed using a peak fit program (Origin software, OriginLab Corporation, Northampton, MA). The size of the G and the M1 peaks were calculated as the peak area (%) relative to the overall G + M1 peaks.

2.3. Proton NMR relaxation study

NMR relaxation measurements were performed on a Bruker Avance DRX-500 spectrometer (Bruker Instrument, Inc., Billerica, MA) operating at a proton resonance frequency of 500 MHz. A 5 mm diameter NMR sample tube was used. T_2 values of water protons were measured using the Carr–Purcell–Meiboom–Gill (CPMG) pulse sequence. Acquisition parameters were as follows, 90° pulse of 8–9 μs, relaxation delay of 10 s, and 90–180° pulse spacing of 100–250 μs, depending on water content of the system. The probe was equipped with a programmable heating and cooling control. In order to deconvolute the G and the M1 processes, the sample was heated and cooled in the NMR probe as shown in Fig. 3. Relaxation curves obtained from the CPMG pulse sequence were analyzed as a continuous distribution of exponentials with Gendist software (Robert Johnson, Uppsala University, Sweden). The program is based on the REPES algorithm to perform the inverse Laplace transform convolution (Jakes, 1995). All measurements were done in duplicate.

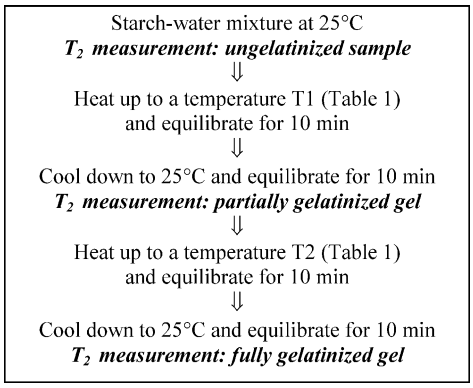

Fig. 3. Temperature program for the NMR relaxation study.

For ungelatinized starch–water systems, the amount of each water population in the T_2 distribution spectrum was calculated using the following equation

$$w_i = (A_i/A_{total}) \times (w_w/w_{ds}) \quad (5)$$

where w_i is the amount of water population (g water/g dry starch) associated with peak i in the relaxation spectrum. A_i and A_{total} represent the area under peak i and sum of the area of all peaks in the spectrum, respectively. w_w/w_{ds} is the ratio between weight of water and starch, or initial water content (g water/g dry starch) of the system.

3. Results and discussion

3.1. DSC studies of frozen and additional unfrozen water of starch–water mixtures

Our results show that the amount of frozen water is linearly related to the initial water content of the system, with a slope close to 1 ($R^2 > 0.99$, data not shown). UW can be obtained from the x-intercept of the plot of the initial water content against FW (Table 2). Our UW results for ungelatinized starches are close to those in the literature (Wootton and Bamunuarachchi, 1978), which are 0.32, 0.30 and 0.38 g water/g dry starch for waxy corn, normal corn and potato starches, respectively. UW of all hydrated starches clearly increases after being heated, suggesting an increase in an extent of hydration due to gelatinization. The values in Table 2 are based on the assumption that UW and AUW are not dependent on the initial water content of the system. However, the calculation of AUW using Eqs. (1)–(3) suggests that this assumption may not be true. AUW appears to depend on the water content of the mixture (Fig. 4). In most cases, as water content increases, AUW increases to maximum, then decreases.

An explanation for the variation of AUW with different initial water contents could be suggested by a consideration of the changes in the starch–water interactions within a gel

Table 2
The amount of UW and AUW in different starch–water mixtures

Type of starch	Amount of UW (g water/g dry starch) at different stages			Amount of AUW (g water/g dry starch)	
	Ungelatinized (UW1)	Partially gelatinized[a] (UW2)	Fully gelatinized[b] (UW3)	G endotherm (UW2–UW1)	M1 endotherm (UW3–UW2)
Waxy corn	0.347±0.004	0.360±0.003	0.442±0.004	0.013±0.001	0.082±0.003
Normal corn	0.332±0.003	0.342±0.002	0.419±0.004	0.011±0.001	0.077±0.003
Potato	0.429±0.003	0.434±0.004	0.457±0.004	0.005±0.001	0.023±0.002
Pea	0.355±0.003	0.365±0.003	0.396±0.002	0.010±0.000	0.031±0.001

[a] Heat to a temperature T1 (Table 1).
[b] Heat to a temperature T2 (Table 1).

network. In a starch–water mixture, water of hydration can be found near the surface of starch polymers. Water molecules in this environment may have different physical properties from those of pure water due to their interactions with the macromolecules, and could remain unfrozen at subzero temperature. During freezing, it is thermodynamically unfavorable to move these hydration waters to form ice clusters due to the water–polymer interactions and the involvement of water in the zone of the polymer structure. The extent of the hydration depends on several factors including distance of water molecules from the surface of polymers. In the case of membranes and macromolecules, as distance from the surface increases, the work needed to remove the hydrated water decreases exponentially (Wolfe, Bryant, & Koster, 2002). Properties of the surface, particularly its charge and the area density of hydrogen bonds, also affect the degree of hydration (Wolfe et al.). The structural conserving function of UW is mainly driven by the relatively immobile state of polymer chains under the prevailing conditions in a frozen system. If hydration water should migrate to form ice, rearrangement of the polymer structure would be necessary to adjust to the loss of those water molecules. However, this situation is unfavorable since considerable energy will be required to

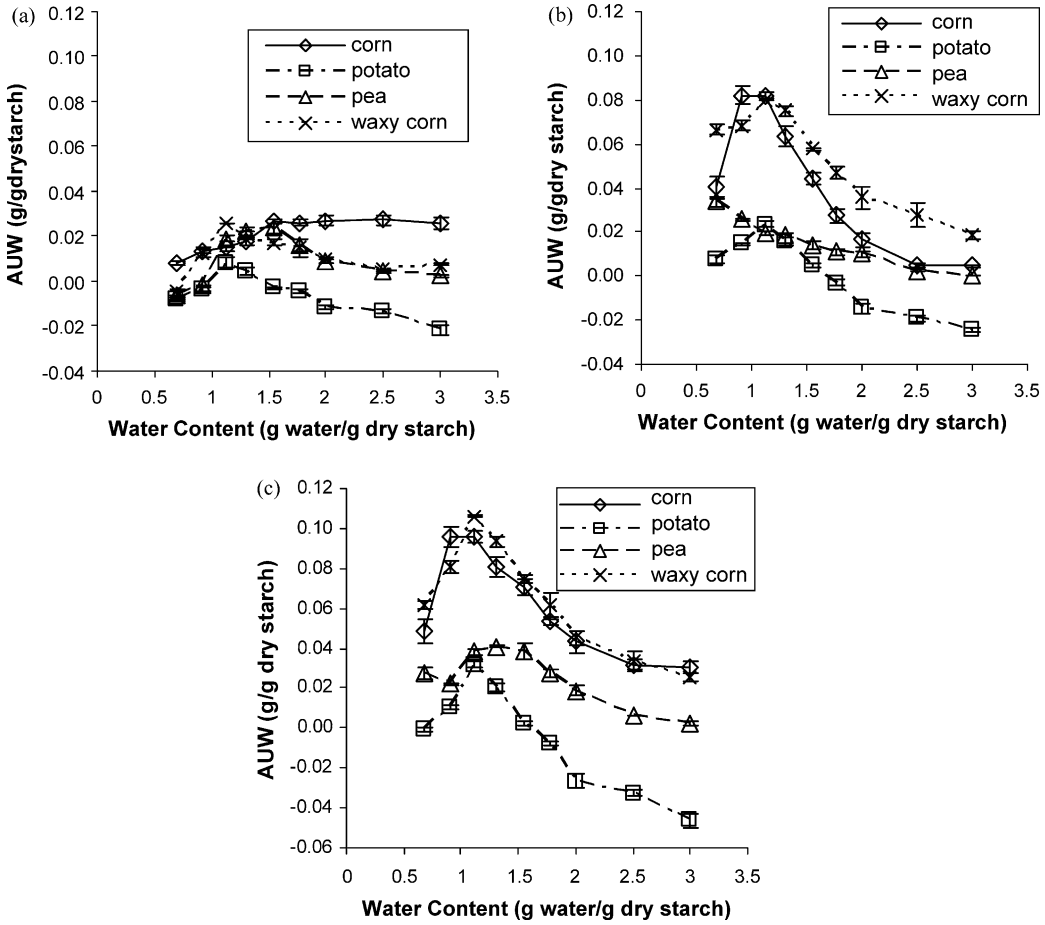

Fig. 4. Effect of water content on AUW_G (a), AUW_{M1} (b), and AUW_{G+M1} (c). Error bars extend one standard deviation above and below the mean.

alter the polymer conformation at subzero temperature. Therefore, a sufficient amount of UW is retained in the system. Changing the total water content would influence the overall gel structure, thus altering the magnitude and extent of starch–water interactions and the arrangements of disrupted amylose and amylopectin clusters. The maximum AUW of most starches is found for a water content which corresponds to a semi-solid, saturated suspension with little or no additional supernatant water. In this condition, the extra-granular water has been proposed to exist as a thin layer between closely packed granules (Tang et al., 2000). The gel structure of those concentrated starch systems has also been described as a tightly packed system of swollen granules with a thin layer of amylose gel between the granules (Garcia, Colonna, Bouchet, & Gallant, 1997; Keetels, van Vliet, & Walstra, 1996). It is thus proposed that such a 'dense' gel matrix would be characterized by there being a short distance between hydration waters and starch polymers, and also a high local volume density of hydrogen bonds, which might mitigate against the migration of hydration water to form ice, resulting in the maximum AUW observed. As the initial water content increases, AUW of the systems tends to decrease, indicating reduced starch–water interactions presumably due to a more 'swollen' (hence less 'dense') gel network. In this case, the increased distance between the polymer surfaces and the larger clusters of contiguous water molecules would facilitate ice formation, resulting in the lower AUW formed.

The maximum heating temperature also affects the degree of starch–water interactions. Starch–water systems heated to the temperature of completion of the M1 endotherm tend to show an increase in AUW compared to the partial gelatinization condition (G endotherm; Fig. 4a and b). This result suggests that more water molecules are absorbed into the polymer matrix after subjecting it to a higher temperature. Previous studies have shown that a significant reduction in the crystallinity levels of starch granules occurs at temperatures higher than the peak temperature of the G endotherm (Jenkins & Donald, 1998; Le Bail et al., 1999; Svensson & Eliasson, 1995). As the granule structure becomes increasingly disrupted at higher temperatures, more starch polymers, especially amylopectin, could be disentangled and expose more hydroxyl groups to water, resulting in increased starch–water interactions. The magnitude of AUW is also dependent on type of starch used. Fig. 4 shows an intermediate AUW for pea starch compared to waxy corn, normal corn and potato starches. The C-polymorph in pea starch consists of a mixture of A- and B-types. Therefore, its gelatinization behavior is

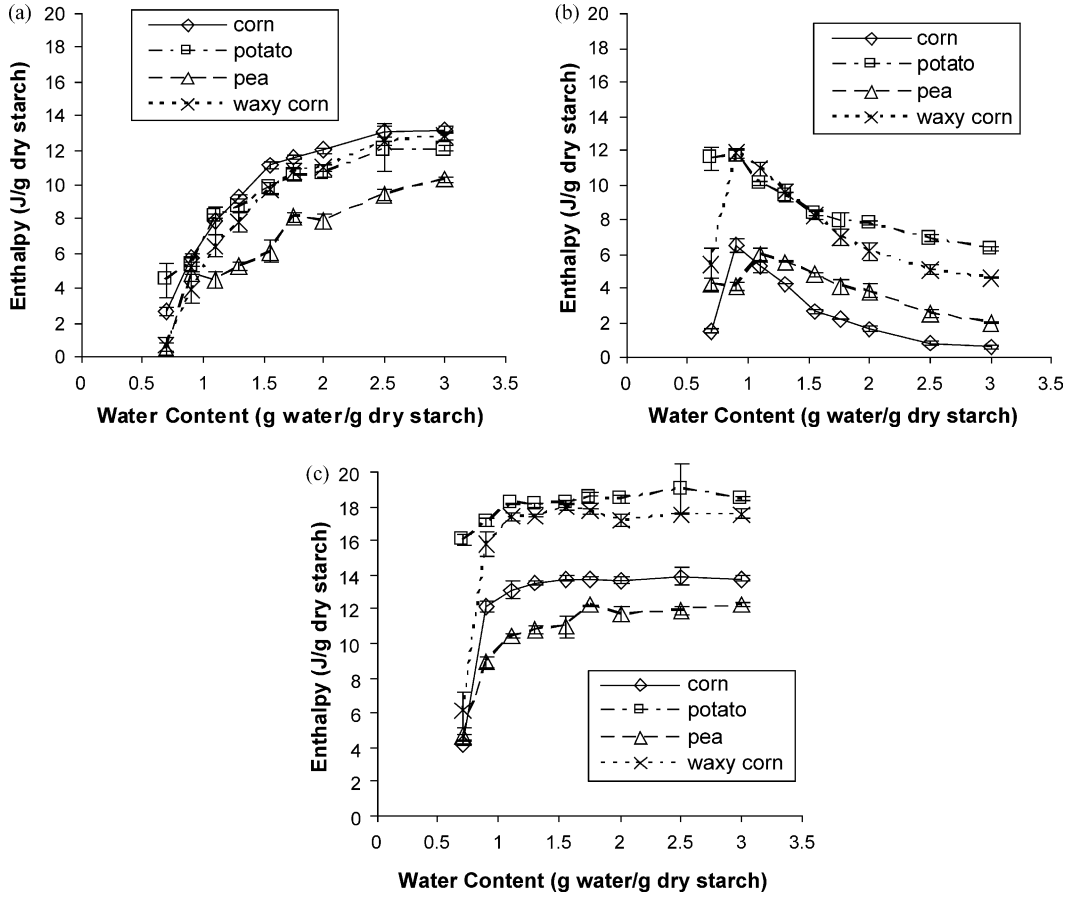

Fig. 5. Effect of water content on $\Delta H_{gel,G}$ (a), $\Delta H_{gel,M1}$ (b) and $\Delta H_{gel,G+M1}$ (c). Error bars extend one standard deviation above and below the average.

expected to be intermediate between those of corn and potato starches. The results of AUW correspond to this expectation. Despite the different amylose content among waxy corn (0% amylose) and the other type of starches (25–35% amylose), all the starch types show relatively similar trend of the change in AUW as a function of the initial water content, especially after the complete gelatinization (Fig. 4b and c). This might imply an important role of amylopectin in governing the interactions between water and gelatinized starches.

3.2. Gelatinization endotherms of different starch–water systems

The DSC deconvolution technique reveals that the magnitude of the G and the M1 endotherms is dependent on the initial water content (Fig. 5a and b) while the overall gelatinization endotherm (G+M1) stays constant when the water content is higher than 0.9 g water/g dry starch (Fig. 5c). At water contents beyond 1.5 g water/g dry starch at which only the G endotherm is apparent, the instrumental deconvolution still provides a small value of ΔH_{gel} in the rescanned thermogram. According to Blanshard (1987), the disappearance of the M1 endotherm at the excess water condition could be considered as the convolution of the M1 with the G peak. Therefore, we postulate that the small endotherm in the rescanned thermogram is the M1 endotherm. The overall results in Fig. 5 suggest that, as the water content increases, the G process becomes more dominant while the extent of the M1 process is much reduced. Eventually, the M1 process overlaps with the G process, resulting in one apparent endothermic peak. Comparing this instrumental deconvolution to the conventional mathematical deconvolution, our instrumental deconvolution gives similar results in terms of the relative peak area of the G and the M1 endotherms although the position of the M1 peak from the real DSC thermogram is not the same as the one from the software deconvolution (Figs. 6 and 7, only the results from waxy corn starch are shown). These results suggest that stopping the DSC scan near the peak temperature of the G endotherm is sufficient to eliminate the G endotherm, as is to be expected from the characteristics of a thermally induced process.

The nature of the processes of the G and the M1 endotherms has been generally hypothesized to be associated with solvent-assisted structural disruption. Although a number of mechanisms have been suggested, there were three classical models advanced in the literature. The first model, proposed by Donovan (1979), focuses on changes in an individual granule assumed representative of the system.

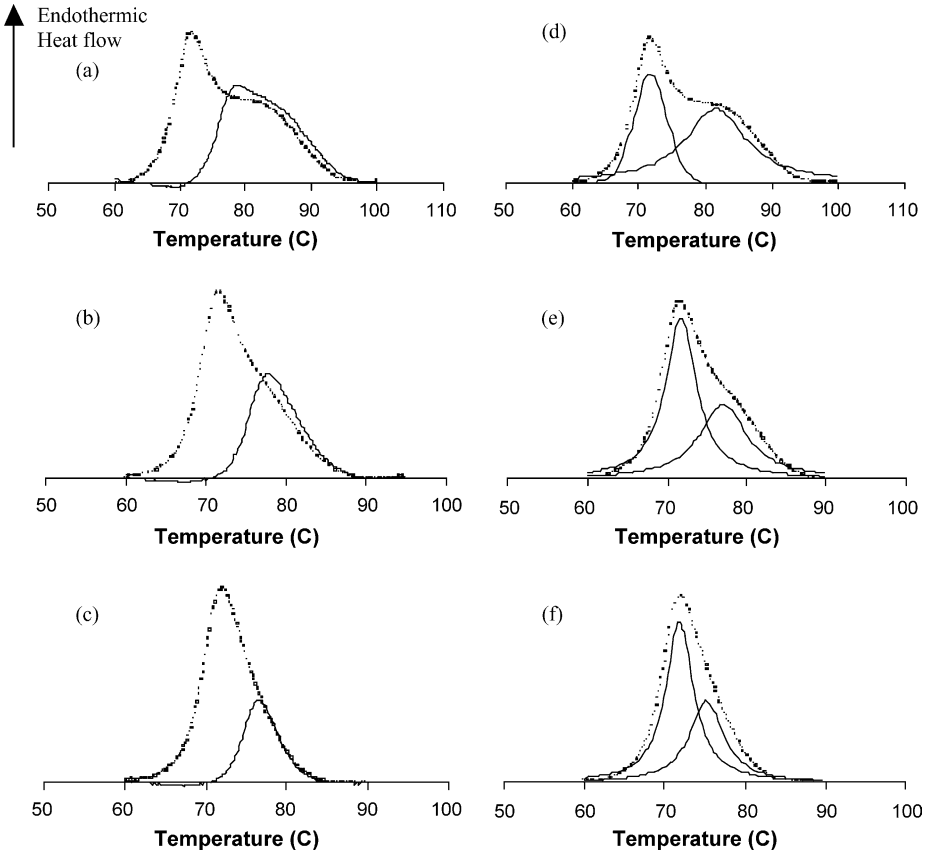

Fig. 6. The complete DSC thermogram (G+M1, dotted lines) of waxy corn starch at different water content, 1.1 g water/g dry starch (a, d), 1.5 g water/g dry starch (b, e), and 2.0 g water/g dry starch (c, f), with the deconvoluted peaks (straight lines) from the instrumental deconvolution, showing the M1 endotherm (a–c), and from the mathematical curve fitting technique, showing both G and M1 endotherms (d–f).

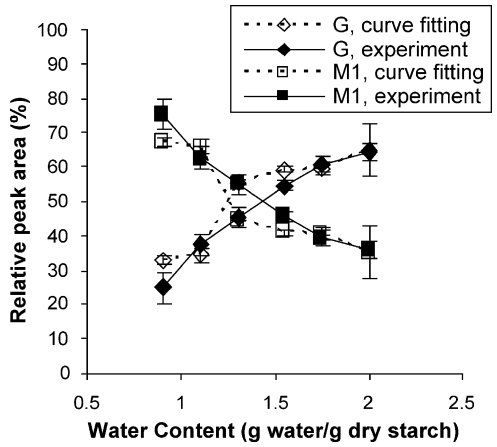

Fig. 7. Relative peak area of the G and the M1 endotherms of waxy corn starch, calculated from the instrumental deconvolution and the mathematical curve fitting techniques.

The starch–water interactions are thought to start mainly in amorphous regions of the granule. The first gelatinization peak (G endotherm) has been suggested to result from the swelling-driven crystalline disruption, in which the swelling of the amorphous regions is considered to 'strip' polymer chains from the surface of crystallites, while the second peak (M1 endotherm) represents the melting of the remaining less hydrated crystallites. Since this model, solely based on DSC data, had scant supporting evidence, it has been revised (Blanshard, 1987) and tested with additional instrumental approaches (Jenkins & Donald, 1998). A second model, proposed by Evans and Haisman (1982) considers the system as a population of starch granules with a range of properties. The successive gelatinization peaks have been suggested to reflect the melting of the crystallites with different stabilities due to a gradient of water within the sample. The G endotherm represents the highly cooperative melting of crystallites initiated by those with least stability. Increased amounts of available water facilitate the gelatinization by lowering the melting point of the remaining crystallites. As the water becomes limiting, most of the water molecules are absorbed by the disordered polysaccharide chains, resulting in insufficient remaining water to facilitate the melting of more stable crystallites. Hence, a higher temperature is needed to melt these remaining crystallites, causing the M1 endotherm to become evident. This postulate has been supported by subsequent studies (Cruz-Orea, Pitsi, Jamée, & Thoen, 2002; Garcia et al., 1997; Liu & Lelievre, 1992; Liu, Lelievre, & Ayoungchee, 1991). A third model, proposed by Slade and Levine (1988), applies the glass transition concept to explain the gelatinization phenomena. In this model, the G endotherm is considered to reflect primarily plasticization in amorphous region, which is required before initiation of the melting of crystallites, and the M1 endotherm reflects non-equilibrium melting of crystallites. In limited water conditions, the effective glass transition temperature (T_g) of the amorphous regions becomes higher, resulting in an elevated effective melting temperature (T_m) of crystalline region. Therefore, gelatinization can be observed as two endothermic events. Adding water reduces the T_g value of the amorphous region, facilitating crystalline disruption at a lower temperature, leading to apparently one gelatinization endotherm. However, there is disagreement as to the location of T_g, which might not correspond to the temperature of the leading edge of the first DSC peak as proposed in this model (Liu & Lelievre, 1991; Liu et al., 1991).

Considering all three models, the first and the third suggest that gelatinization is initiated in the amorphous region, then continues as crystalline disruption. In contrast, the second model does not attribute any particular significance to the amorphous region, but attributes the whole process only to changes in the crystalline region. This may not provide the whole picture of the gelatinization process. Considering the system as a population of starch granules, the first model assumes that all granules are identical in terms of swelling capability and stability of crystallites, whereas the concept of the varied crystalline stability among granules, set forth in the second model, results in different gelatinization behaviors for different granules. The second model appears to better conform to the observation of 'competitive gelatinization' among starch granules (all granules do not gelatinize promptly), usually seen in light microscope. A more detailed comparison of all aspects of the three models indicates that none gives entirely satisfactory overview of the gelatinization mechanism. Moreover, these models do not provide a detailed description of the structural change during gelatinization. Recently, based on DSC, SAXS, SANS, dynamic mechanical analysis, optical microscopy and NMR data, Waigh, Gidley, Komanshek, and Donald (2000) have proposed a new mechanism, focusing on the change in the crystalline structure during gelatinization. This recent model considers amylopectin molecules to be a side-chain liquid–crystalline polymer. Gelatinization is described as the coupling between self-assembly, described as the dissociation of amylopectin double helices side-by-side (helix–helix dissociation), and the breakdown of the overall crystalline structure during heating. Providing an explicit molecular mechanism for the 'swelling driven processes', the self-assembly can be viewed as an indicator of solvent ingress, which subsequently produces swelling of the crystalline growth rings. At intermediate water contents (5–40%, w/w), the G endotherm is considered to reflect the helix–helix dissociation whereas the M1 endotherm is a result of the helix–coil transition of amylopectin helices. In excess water (>40%, w/w), it can be considered that both the helix–helix dissociation and the helix–coil transition occur simultaneously. The endotherms therefore merge together. An effect of amylopectin crystallinity structure on the gelatinization mechanism is also included in this model. Based on Zimm/Bragg theory of helix–coil transitions, the breadth of the thermodynamic transition is expected to be inversely proportional to the double helix length. Therefore,

A-type starches with shorter amylopectin double helices exhibit a broader M1 endotherm than B-type starches. This is in addition to the realization regarding the effect of the chain length (involved in the crystalline unit) on the gelatinization temperature. The longer the chain length, the higher will be the expected gelatinization temperature (Moates, Noel, Parker, & Ring, 1997; Whittam, Noel, & Ring, 1990).

The variation of the ΔH_{gel} among different starches (Fig. 5) might result from several factors. Although pea starch has a composite A- and B-type crystallinity, ΔH_{gel} of pea starch tends to be lower than that of waxy corn, normal (wild-type) corn and potato starches. Since ΔH_{gel} can be considered to represent the energy required to disrupt both crystallinity and molecular order (double helical association) (Bogracheva, Wang, Wang, & Hedley, 2002; Cooke & Gidley, 1992; Waigh et al., 2000), the qualitative determination of the amylopectin crystallinity might not be sufficient in itself to explain the variation in ΔH_{gel}. A study by Bogracheva et al. (2002) has shown that, at similar water contents, wild-type pea starch has a lower amount of crystalline amylopectin and a lower proportion of double helical material than does waxy corn starch. Wild-type pea starch also contains a lower double helical content than wild-type potato starch. These differences might contribute to a lower ΔH_{gel} of pea starch compared to that of waxy corn and potato starch. However, the amount of crystalline amylopectin and double helical content of wild-type pea starch are closer to those of wild-type corn starch (Bogracheva et al., 2002), which is in accordance with smaller difference between their ΔH_{gel}, especially for the M1 and the G+M1 endotherms. A difference in ΔH_{gel} can also be found between the starches with the same type of amylopectin crystallinity. Our results show that waxy corn starch has higher $\Delta H_{gel,M1}$ and $\Delta H_{gel,G+M1}$ as compared to its amylose-containing counterpart (Fig. 5b and c), presumably due to its higher percentage of crystallinity (Cooke & Gidley, 1992; Bogracheva et al., 2002.; Cheetham & Tao, 1998b) as well as a higher proportion of double helices (Cooke & Gidley, 1992; Bogracheva et al., 2002; Gidley & Bociek, 1985). A third factor may be the lack of amylose–lipid inclusions in the granules. It has been proposed that an exothermic effect from the formation of amylose–lipid complexes, which could occur during gelatinization (Le Bail et al., 1999), might contribute to the reduction of the apparent ΔH_{gel} of lipid-containing starches (Biliaderis, Page, Maurice, & Juliano, 1986; Rolee, Chiotelli, & Le Meste, 2002). Melting of the amylose–lipid complexes is usually observed as a reversible endothermic transition following the gelatinization endotherm. For lipid-containing cereal starches, this reversible endotherm can be seen near 100 °C in excess water (>1.5 g water/g dry starch) (Le Bail et al., 1999). However, the amylose–lipid complex melting peak was not observed in this study since the DSC scans were stopped a few degrees above the end of the M1 endotherm. In excess water, the reported values of the melting enthalpy of amylose–endogenous lipid complexes of wild-type cereal starches range between 1.0 and 3.0 J/g starch, wet basis (Biliaderis et al., 1986; Kugimiya, Donovan, & Wong, 1980; Morrison, Tester, Snape, Law, & Gidley, 1993; Vilwock, Eliasson, Silverio, & BeMiller, 1999). Due to the reversible nature of amylose–lipid complex formation and melting, the melting enthalpy might partly be responsible for the difference between $\Delta H_{gel,G+M1}$ of waxy corn and normal corn starch, which is approximately 4 J/g dry starch (Fig. 5c). Considering the magnitude of ΔH_{gel} of complete gelatinization, our results are close to the values previously reported (Bogracheva et al., 2002; Jane et al., 1999; Kim, Wiesenborn, Orr, & Grant 1995).

3.3. Proton NMR relaxation study of different starch–water mixtures

The distribution of water protons T_2 reveals two distinct water populations in the ungelatinized starch–water mixtures (Fig. 8). The positions of the peaks with the lower T_2 range, reflecting the lower mobility, are independent of the initial water content, whereas the peaks with the higher T_2 range (more mobile water fraction) show an increase in T_2 as the water content increases (Figs. 8 and 9). Based on an assumption that the diffusive exchange of water molecules between two distinct regions is slow on the NMR timescale, the relative peak areas of these relaxation spectra should be proportional to the relative water populations (Tang et al., 2000). Hence, the amounts of the less mobile and the more mobile water, denoted as w_a and w_b, respectively, may be calculated using Eq. (5). Fig. 10 shows that only w_b is dependent on the initial water content. These results suggest that the less mobile water fraction occupies a more constant or unchanged environment, probably the interior of the granule. The increase in the T_2 of the more mobile water peak (T_{2b}) and w_b as initial water content increases suggests that this mobile water fraction is related to the bulk water phase, exterior to the granule.

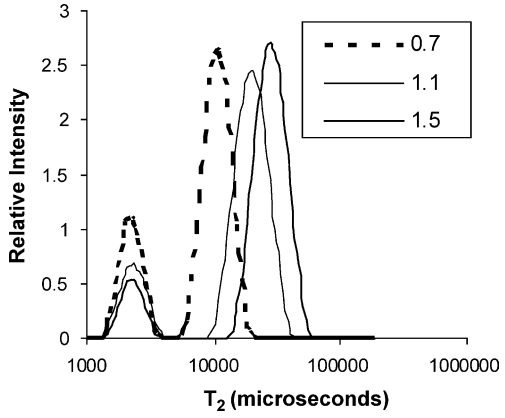

Fig. 8. T_2 distribution for ungelatinized normal corn starch–water systems at different water contents, 0.7, 1.1 and 1.5 g water/g dry starch.

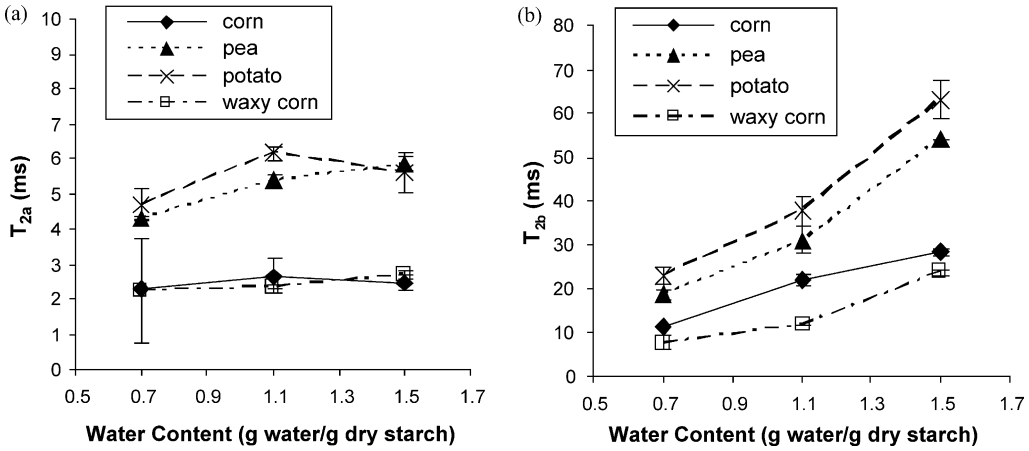

Fig. 9. T_2 of the peaks as a function of initial water content for different starch–water mixtures: (a) less mobile water fraction (T_{2a}); (b) more mobile water fraction (T_{2b}). Error bars extend one standard deviation above and below the average.

Based on the assumption that water within different compartments is distinguishable in an NMR relaxation study only if the rate of diffusive exchange of water molecules between two distinct regions is low compared to their intrinsic relaxation rates, a relationship between water distribution and starch granule microstructures has been reported (Chatakanonda, Chinachoti et al., 2003; Tang et al., 2000, 2001). By monitoring the temperature dependence of the T_2 distribution of water protons for a saturated packed bed (1.1 g water/g dry starch), ungelatinized potato starch granules, three distinct water populations, assigned to extra-granular water, water in the amorphous growth rings and water in the amorphous regions of the crystalline lamellae, have been identified. The first water population is clearly seen at 17 °C as a peak with T_2 centered around 50 ms. The short T_2 of this water external to granules compared to a T_2 of 3 s for bulk water might be the result of chemical exchange with hydroxyl protons of the starch polymers on the granule surface. The other two populations representing 'intra-granular' water are in fast diffusional exchange at 17 °C, and exhibit a single peak with T_2 centered around 8 ms. These intra-granular water populations slowly exchange with the extra-granular water and may also chemically exchange with hydroxyl protons of the starch polymers. As the system is cooled down to 4 °C, the two populations of the intra-granular water enter slow exchange regime, resulting in two distinct peaks (Tang et al., 2000). Comparing our T_2 distribution with the results from Tang et al. (2000), the less mobile water population could be assigned as the intra-granular water whereas the more mobile water population could represent the extra-granular water. These identifications are in a good agreement with the relationship of each water fraction on the total water content in the system. An ungelatinized starch granule can retain a certain amount of intra-granular water in the reversible swelling condition (Hoseney, 1998). Additional water mainly stays outside the granule. An increase in the total water content of the system thus does not produce a significant effect on the less mobile intra-granular water, though it strongly influences the relaxation behavior

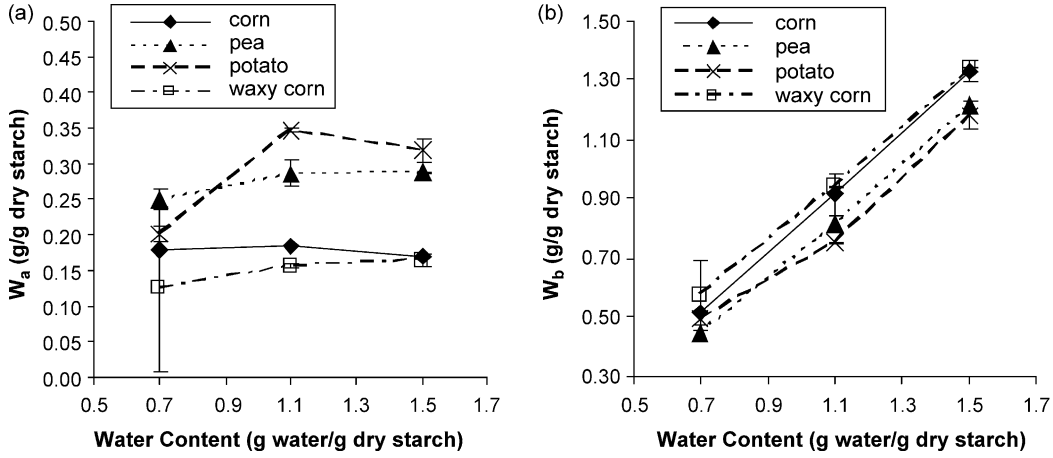

Fig. 10. Amount of different water fractions as a function of initial water content for different starch–water mixtures: (a) less mobile water fraction (w_a); (b) more mobile water fraction (w_b). Error bars extend one standard deviation above and below the average.

as well as the amount of the more mobile extra-granular water. Considering the less mobile water fraction, differences in its T_2 (T_{2a}) and its amount (w_{2a}) are observed among different starch types (Figs. 9a and 10a), implying an effect of the type of amylopectin polymorph. Waxy corn and normal corn starches exhibit similar T_{2a} and w_{2a} presumably due to the same A-type polymorph. T_{2a} and w_{2a} of the C-type pea starch are intermediate between those of A- and B-type starches, corresponding to its composite A- and B-type structures.

The dynamic redistribution of extra- and intra-granular water in starch–water systems (at water content 1.1 g water/g dry starch) at different extents of gelatinization is shown in Fig. 11. The overall results show that being exposed to the heating process enhances the diffusive exchange of water between the two regions. This may be caused by structural disruption during heating. After partial gelatinization, some of the structural barriers have been destroyed, leading to a faster exchange of water molecules between different regions as shown by either a reduction in the less mobile water fraction or the merging of the two peaks into one peak. As the maximum heating temperature is increased, the accompanying extensive structural disruption may result in a reduced degree of heterogeneity in the system. Only one water fraction, resulting from fast diffusional averaging, with a sharp T_2 distribution, is observed in the gel that has undergone the M1 process. Previous NMR diffusometry in hydrated potato starch (1.1 g water/g dry starch) has shown that destruction of the granule structure after full gelatinization changes the diffusion of water molecules from two-dimensional diffusion in an ungelatinized system to an unrestricted three-dimensional diffusion in a starch gel (Hills, Godward, Manning, Biechlin, & Wright, 1998). A similar pattern of water redistribution after gelatinization was also observed from all types of starch with 0.7 and 1.5 g water/g dry starch (data not shown).

T_2 values of peaks due to water protons in the starch gels are affected by several factors (Table 3). A decrease in T_2 is observed when the water content decreases, corresponding to the results of a recent NMR relaxation study in wheat starch gels (Choi & Kerr, 2003). This could be explained by the existence of a relatively larger fraction of water having a reduced mobility. In a more concentrated gel, water molecules are likely to reorient more slowly as they are more extensively hydrogen bonded to relatively large and immobile starch polymers. Also, cross-relaxation and chemical exchange between water protons and starch hydroxyl protons might be enhanced in the concentrated

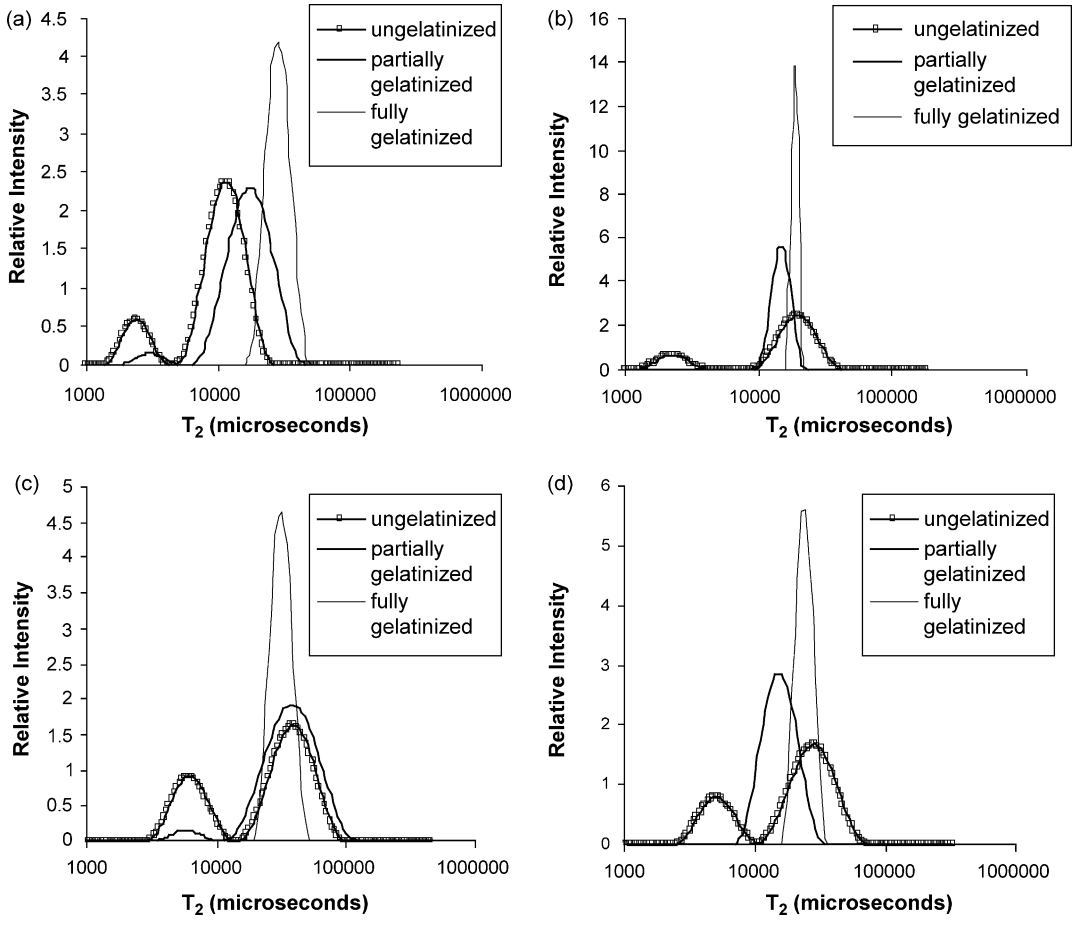

Fig. 11. T_2 distribution for different starch gels, 1.1 g water/g dry starch, at 25 °C: (a) waxy corn starch; (b) normal corn starch; (c) potato starch; (d) pea starch.

Table 3
T_2 of the peaks, measured at 25 °C, for different starch gels

Starches	T_2 of the peaks (ms)					
	0.7 g water/g dry starch		1.1 g water/g dry starch		1.5 g water/g dry starch	
	Partially gelatinized[a]	Fully gelatinized[b]	Partially gelatinized	Fully gelatinized	Partially gelatinized	Fully gelatinized
Waxy corn[c]	9.80±0.99[d]	15.20±1.98	17.40±0.00	30.20±1.98	49.00±1.41	67.60±2.26
Corn	7.60±0.00	7.30±2.55	15.00±0.00	18.50±0.71	21.45±0.64	25.05±0.07
Pea	10.75±0.35	14.85±2.62	16.60±1.13	26.40±3.39	32.80±7.07	55.55±2.05
Potato[c]	19.50±0.71	17.60±1.27	38.15±2.62	30.20±1.98	58.50±2.12	56.00±1.41

[a] Heat to a temperature T1 (Table 1).
[b] Heat to a temperature T2 (Table 1).
[c] Although two water fractions were observed in the partially gelatinized gels, only T_2 values of the more mobile water fraction was reported here.
[d] Represent one standard deviation from means.

polymer system, leading to a faster relaxation process (Hills, Takacs, & Belton, 1990; Yakubu, Ozu, Baianu, & Orr, 1993). Considering the effects of the maximum heating temperature, the T_2 values for the fully gelatinized starch gels are either similar to or higher than those of the partially gelatinized gels. According to the DSC studies, at 0.7, 1.1 and 1.5 g water/g dry starch, AUW from the M1 process is greater than that of the G process, suggesting enhanced starch–water interactions (Fig. 4a and b). Therefore, water might be expected to be less mobile in the fully gelatinized gels. However, our results do not conform to this expectation. This might partly be due to the effect of the mobility of starch polymers on the relaxation process of water protons. Since T_2 of exchangeable water protons could be greatly influenced by chemical exchange of the water protons with the hydroxyl protons in the starch polymers, the T_2 distribution of water protons could reflect a dynamic state of starch chains (Tang et al., 2001). Earlier NMR relaxation studies of a D_2O-saturated packed bed of potato and cassava starches, which mainly reflect the mobility of the non-exchanging starch CH protons, have reported a progressive increase in the relative peak area associated with the more mobile amylose/amylopectin molecules, indicating the increasing mobility of the starch polymers associated with the plasticization and/or melting, as temperature increases (Chatakanonda, Chinachoti et al., 2003; Tang et al., 2001). In a fully gelatinized gel, a greater degree of structural disruption might result in more flexible, disentangled starch polymers exhibiting the longer T_2 of exchangeable starch hydroxyl protons, and the exchanging water protons. In addition, a larger T_2 might be related to the fact that water molecules have a longer distance to diffuse before achieving interaction with the polymer surfaces (Choi & Kerr, 2003). This might occur in fully gelatinized gels with less of a structural barrier. The differing microstructures of the starch gels are another important factor that is apparently involved in the relaxation behavior of water proton in the systems. T_2 of pea starch gels falls in between that of normal corn and potato starch gels (Table 3). This might relate to its original C-type polymorph, which is suggested to have a gel structure with combined characteristics of those from A- and B-type starches.

4. Conclusion

Starch–water interactions during gelatinization are greatly influenced by the initial water content, the highest heating temperature, as well as the microstructures of starch granules and the gel matrix. Using the deconvolution DSC method, the extent of the interactions could be estimated by measuring AUW, which reflects the greater degree of hydration after the gelatinization process. AUW largely depends on the initial water content. At the water content providing maximum AUW, the resulting 'dense' gel matrix might increase the degree of hydration. Thus, the migration of the hydration water to form ice inclusions is extremely unfavorable. Starch–water systems heated up to higher temperatures have larger AUW, which might result from a larger extent of structural disruption. Deconvolution of the G and the M1 endotherms suggests that both endotherms gradually overlap as water content increases, presumably due to water-assisted, cooperative gelatinization. The different ΔH_{gel} values among different types of starch might not be adequately explained as resulting from different amylopectin crystallinity types. Several other factors might be involved, including the proportion of double helices, the level of crystallinity and the present of amylose–lipid inclusions. Water proton NMR relaxometry successfully reveals a dynamic redistribution of the intra- and the extra-granular water during gelatinization. Full gelatinization results in an apparently homogeneous gel, with a single water fraction from fast diffusional averaging observed. For pea starch, AUW as well as the T_2 values of the peaks are in the intermediate between those of corn and potato starches, corresponding to its categorized as containing a mixture of A- and B-type polymorphs.

References

Biliaderis, C. G., Page, C. M., Maurice, T. J., & Juliano, B. O. (1986). Thermal characterization of rice starches: A polymeric approach to phase transitions of granular starch. *Journal of Agricultural and Food Chemistry*, *34*, 6–14.

Blanshard, J. M. V. (1987). Starch granule structure and function: A physicochemical approach. In T. Gallard (Ed.), *Starch: Properties and potential* (pp. 16–54). Chicester: Wiley.

Bogracheva, T. Y., Wang, Y. L., Wang, T. L., & Hedley, C. L. (2002). Structural studies of starches with different water contents. *Biopolymers*, *64*, 268–281.

Chatakanonda, P., Chinachoti, P., Sriroth, K., Piyachomkwan, K., Chotineeranat, S., Tang, H. R., & Hills, B. (2003). The influence of time and conditions of harvest on the functional behavior of cassava starch—a proton NMR relaxation study. *Carbohydrate Polymers*, *53*, 233–240.

Chatakanonda, P., Dickinson, L. C., & Chinachoti, P. (2003). Mobility and distribution of water in cassava and potato starches by ^{1}H and ^{2}H NMR. *Journal of Agricultural and Food Chemistry*, *51*, 7445–7449.

Cheetham, N. W. H., & Tao, L. (1998a). Oxygen-17 NMR relaxation studies on gelatinization temperature and water mobility in maize starches. *Carbohydrate Polymers*, *35*, 279–286.

Cheetham, N. W. H., & Tao, L. (1998b). Variation in crystalline type with amylose content in maize starch granules: An X-ray powder diffraction study. *Carbohydrate Polymers*, *36*, 277–284.

Chinachoti, P., White, V. A., Lo, L., & Stengle, T. R. (1991). Application of high-resolution carbon-13, oxygen-17 and sodium-23 nuclear magnetic resonance to study the influences of water, sucrose, and sodium chloride on starch gelatinization. *Cereal Chemistry*, *68*, 238–244.

Choi, S. G., & Kerr, W. L. (2003). Water mobility and textural properties of native and hydroxypropylated wheat starch gels. *Carbohydrate Polymers*, *51*, 1–8.

Cooke, D., & Gidley, M. J. (1992). Loss of crystalline and molecular order during starch gelatinization: Origin of the enthalpic transition. *Carbohydrate Research*, *227*, 103–112.

Cruz-Orea, A., Pitsi, G., Jamée, P., & Thoen, J. (2002). Phase transitions in the starch–water system studied by adiabatic scanning calorimetry. *Journal of Agricultural and Food Chemistry*, *50*, 1335–1344.

Donovan, J. W. (1979). Phase transition of the starch–water system. *Biopolymers*, *18*, 263–275.

Evans, I. D., & Haisman, D. R. (1982). The effect of solutes on the gelatinization temperature range of potato starch. *Starch*, *34*, 224–231.

Franks, F. (1986). Unfrozen water: Yes; unfreezable water: hardly; bound water: certainly not. *Cryo-Letters*, *7*, 207.

Garcia, V., Colonna, P., Bouchet, B., & Gallant, D. J. (1997). Structural changes of cassava starch granules after heating at intermediate water contents. *Starch*, *49*, 171–179.

Gidley, M. J., & Bociek, S. M. (1985). Molecular organisation in starches: A ^{13}C CP/MAS NMR study. *Journal of the American Chemical Society*, *107*, 7040–7044.

Hills, B. P., Godward, J., Manning, C. E., Biechlin, J. L., & Wright, K. M. (1998). Microstructural characterization of starch systems by NMR relaxation and Q-space microscopy. *Magnetic Resonance Imaging*, *16*, 557–564.

Hills, B. P., Takacs, S. F., & Belton, P. S. (1990). A new interpretation of proton NMR relaxation time measurements of water in food. *Food Chemistry*, *37*, 95–111.

Hoseney, R. C. (1998). Gelatinization phenomena of starch. In M. A. Rao, & R. W. Hartel (Eds.), *Phase/state transitions in foods* (pp. 95–110). New York: Marcel Dekker.

Hoseney, R. C., Zeleznak, K. J., & Yost, D. A. (1986). A note on the gelatinization of starch. *Starch*, *38*, 407–409.

Jakes, J. (1995). Regularized positive exponential sum (REPES) program—a way of inverting laplace transform data obtained by dynamic light scattering. *Collection of Czechoslovak Chemical Communications*, *60*, 1781–1797.

Jane, J., Chen, Y. Y., Lee, L. F., McPherson, A. E., Wong, K. S., Radosavljevic, M., & Kasemsuwan, T. (1999). Effects of amylopectin branch chain length and amylose content on the gelatinization and pasting properties of starch. *Cereal Chemistry*, *76*, 629–637.

Jenkins, P. J., & Donald, A. M. (1998). Gelatinisation of starch—A combined SAXS/WAXS/DSC and SANS study. *Carbohydrate Research*, *308*, 133–147.

Keetels, C. J. A. M., van Vliet, T., & Walstra, P. (1996). Gelation and retrogradation of concentrated starch systems. 3. Effect of concentration and heating temperature. *Food Hydrocolloids*, *10*, 363–368.

Kim, Y. S., Wiesenborn, D. P., Orr, P. H., & Grant, L. A. (1995). Screening potato starch for novel properties using differential scanning calorimetry. *Journal of Food Science*, *60*, 1060–1065.

Kugimiya, M., Donovan, J. W., & Wong, R. Y. (1980). Phase transitions of amylose–lipid complexes in starches: A calorimetric study. *Starch*, *32*, 265–270.

Le Bail, P., Bizot, H., Ollivon, M., Keller, G., Bourgaux, C., & Buléon, A. (1999). Monitoring the crystallization of amylose–lipid complexes during maize starch melting by synchrotron X-ray diffraction. *Biopolymers*, *50*, 99–110.

Lelievre, J., & Mitchell, J. (1975). A pulsed NMR study of some aspects of starch gelatinization. *Starch*, *27*, 113–115.

Li, S., Dickinson, L. C., & Chinachoti, P. (1998). Mobility of 'unfreezable' and 'freezable' water in waxy corn starch by ^{2}H and ^{1}H NMR. *Journal of Agricultural and Food Chemistry*, *46*, 62–71.

Liu, H., & Lelievre, J. (1991). A differential scanning calorimetry study of glass and melting transitions in starch suspensions and gels. *Carbohydrate Research*, *219*, 23–32.

Liu, H., & Lelievre, J. (1992). Differential scanning calorimetry study of melting transitions in aqueous suspensions containing blends of wheat and rice starch. *Carbohydrate Polymers*, *17*, 145–149.

Liu, H., Lelievre, J., & Ayoungchee, W. (1991). A study of starch gelatinization using differential scanning calorimetry, X-ray, and birefringence measurements. *Carbohydrate Research*, *210*, 79–87.

Matveev, Y. I., van Soest, J. J. G., Nieman, C., Wasserman, L. A., Protserov, V., Ezernitskaja, M., & Yuryev, V. P. (2001). The relationship between thermodynamic and structural properties of low and high amylose maize starches. *Carbohydrate Polymers*, *44*, 151–160.

Moates, G. K., Noel, T. R., Parker, R., & Ring, S. G. (1997). The effect of chain length and solvent interactions on the dissolution of the B-type crystalline polymorph of amylose in water. *Carbohydrate Research*, *298*, 327–333.

Morrison, W. R., Tester, R. F., Snape, C. E., Law, R., & Gidley, M. J. (1993). Swelling and gelatinization of cereal starches. IV. Some effects of lipid-complexed amylose and free amylose in waxy and normal barley starches. *Cereal Chemistry*, *70*, 385–391.

Rolee, A., Chiotelli, E., & Le Meste, M. (2002). Effect of moisture content on the thermomechanical behavior of concentrated waxy cornstarch–water preparations—a comparison with wheat starch. *Journal of Food Science*, *67*, 1043–1050.

Rolee, A., & LeMeste, M. (1999). Effect of moisture content on thermomechanical behavior of concentrated wheat starch–water preparations. *Cereal Chemistry*, *76*, 452–458.

Roman-Gutierrez, A. D., Guilbert, S., & Cuq, B. (2002). Frozen and unfrozen water contents of wheat flours and their components. *Cereal Chemistry*, *79*, 471–475.

Slade, L., & Levine, H. (1988). Non-equilibrium melting of native granular starch. Part I. Temperature location of the glass transition associated with gelatinization of A-type cereal starches. *Carbohydrate Polymers*, *8*, 183–208.

Svensson, E., & Eliasson, A. C. (1995). Crystalline changes in native wheat and potato starches at intermediate water levels during gelatinization. *Carbohydrate Polymers*, *26*, 171–176.

Tang, H. R., Brun, A., & Hills, B. (2001). A proton NMR relaxation study of the gelatinisation and acid hydrolysis of native potato starch. *Carbohydrate Polymers*, *46*, 7–18.

Tang, H. R., Godward, J., & Hills, B. (2000). The distribution of water in native starch granules—a multinuclear NMR study. *Carbohydrate Polymers*, *43*, 375–387.

Thomas, D. J., & Atwell, W. A. (1999). *Starches*. St Paul: Eagan Press.

Vilwock, V. K., Eliasson, A. C., Silverio, J., & BeMiller, J. N. (1999). Starch–lipid interactions in common, waxy, *ae du*, and *ae su2* maize starches examined by differential scanning calorimetry. *Cereal Chemistry*, *76*, 292–298.

Waigh, T. A., Gidley, M. J., Komanshek, B. U., & Donald, A. M. (2000). The phase transformations in starch during gelatinisation: A liquid crystalline approach. *Carbohydrate Research*, *328*, 165–176.

Whittam, M. A., Noel, T. R., & Ring, R. G. (1990). Melting behavior of A-type and B-type crystalline starch. *International Journal of Biological Macromolecules*, *12*, 359–362.

Wolfe, J., Bryant, G., & Koster, K. L. (2002). What is 'unfreezable water', how unfreezable is it and how much is there? *Cryo-Letters*, *23*, 157–166.

Wootton, M., & Bamunuarachchi, A. (1978). Water binding capacity of commercial produced native and modified starches. *Starch*, *30*, 306–309.

Yakubu, Y. I., Ozu, E. M., Baianu, I. C., & Orr, P. H. (1993). Hydration of potato starch in aqueous suspension determined from nuclear magnetic studies by ^{17}O, ^{2}H, and ^{1}H NMR: Relaxation mechanisms and quantitative analysis. *Journal of Agricultural and Food Chemistry*, *41*, 162–167.

Yuryev, V. P., Kalistratova, E. N., van Soest, J. G. J., & Niemann, C. (1998). Thermodynamic properties of barley starches with different amylose content. *Starch*, *50*, 463–466.